Supporting Information

A tetracyclic-bislactone-based copolymer donor for efficient semitransparent organic photovoltaics

Mingjie Li,‡[ab] Tai An,‡[bc] Zongliang Ou,[bd] Ke Jin,[bc] Zhiwen Jin,[e] Keyou Yan,[f] He Tian,[g] Wentao Wang,[h] Shangfeng Yang,[i] Guan-Wu Wang,*[a] Qiuling Song,*[d] Zuo Xiao,*[bc] and Liming Ding[bc]

[a] *Hefei National Research Center for Physical Sciences at the Microscale, University of Science and Technology of China, Hefei 230026, China. E-mail: gwang@ustc.edu.cn*
[b] *Center for Excellence in Nanoscience, Key Laboratory of Nanosystem and Hierarchical Fabrication (CAS), National Center for Nanoscience and Technology, Beijing 100190, China. E-mail: xiaoz@nanoctr.cn*
[c] *University of Chinese Academy of Sciences, Beijing 100049, China.*
[d] *Institute of Next Generation Matter Transformation, College of Materials Science & Engineering, Huaqiao University, Xiamen 361021, China. E-mail: qsong@hqu.edu.cn*
[e] *School of Physical Science and Technology, Lanzhou University, Lanzhou 730000, China*
[f] *School of Environment and Energy, South China University of Technology, Guangzhou 510000, China*
[g] *School of Integrated Circuits, Tsinghua University, Beijing 100084, China*
[h] *School of Materials Science and Engineering, Zhejiang Sci-Tech University, Hangzhou 310018, China*
[i] *Department of Materials Science and Engineering, University of Science and Technology of China, Hefei 230026, China.*
‡M. Li and T. An contributed equally to this work.

1. General characterization

NMR spectra were measured on a Bruker Avance-400 spectrometer. Absorption and transmittance spectra were recorded on a Shimadzu UV-1800 spectrophotometer. Cyclic voltammetry was done by using a Shanghai Chenhua CHI620D voltammetric analyzer under argon in an anhydrous acetonitrile solution of tetra-n-butylammonium hexafluorophosphate (0.1 M). A glassy-carbon electrode was used as the working electrode, a platinum-wire was used as the counter electrode, and a Ag/Ag^+ electrode was used as the reference electrode. Polymers were coated onto glassy-carbon electrode and all potentials were corrected against Fc/Fc^+. AFM was performed on a Multimode microscope (Veeco) using tapping mode. The Comission Internationale de l'Eclairage (CIE) 1931 color coordinate and color rendering index (CRI) were obtained by using an Ocean Optics hr2000 spectrophotometer.

2. Synthesis

All reagents were purchased from J&K Co., Aladdin Co., Innochem Co., Derthon Co., SunaTech Co. and other commercial suppliers. N3 was purchased from eFlexPV Co. Dimethyl 2,3-dibromobut-2-enedicarboxylate[1,2] and BDT-Si-Sn[3] were prepared according to literature. All reactions dealing with air- or moisture-sensitive compounds were carried out by using standard Schlenk techniques.

Compound 1. To a stirred solution of thiophen-3-ylboronic acid (4.00 g, 31.3 mmol) in diethyl ether (60 mL) was added 9.7 mL H_2O_2 (30% aqueous solution) at 0 ℃ under nitrogen. Then, the reaction mixture was stirred at room temperature for 1 h. The aqueous layer was extracted with diethyl ether (3 × 30 mL) and the combined ethereal solution was washed with cold saturated aqueous $Na_2S_2O_3$ solution (3 × 30 mL). Removal of ether at 25 ℃ under vacuum gave the intermediate product thiophen-3-ol. To the solution of thiophen-3-ol and N,N-diisopropylethylamine (5.20 g, 40.2 mmol) in anhydrous THF (50 mL) was added bromomethyl methyl ether (5.02 g, 40.2 mmol) dropwise at 0 ℃ over 5 minutes. The reaction mixture was stirred at room temperature for 0.5 h. It was then quenched with water (15 mL) and extracted with CH_2Cl_2 (2 × 20 mL). The combined organic layer passed through a short alkaline alumina column (CH_2Cl_2 as eluent) before being concentrated at 30 ℃ under vacuum. Then, the crude product was purified by alkaline alumina column chromatography (petroleum ether (PE):CH_2Cl_2 = 1:1 as eluent) to yield **compound 1** as a colorless liquid (2.93 g, 65%). Compound 1 was not stable under ambient conditions and was immediately used for the next step reaction. ^{1}H NMR ($CDCl_3$, 400 MHz, δ/ppm): 7.18 (br, 1H), 6.83 (br, 1H), 6.57 (br, 1H), 5.11 (br, 2H), 3.50 (br, 3H). The broadening of the ^{1}H NMR spectrum could be caused by the easy oxidation of compound 1 and the generation of paramagnetic radical species. Due to the instability of compound 1, the ^{13}C NMR spectrum and MS were not acquired.

Compound 2. To a solution of compound 1 (2.93 g, 20.3 mmol) in THF (23 mL) was added *n*-BuLi (1.6 M, 26.4 mmol) at -78 ℃ under nitrogen. After stirring at the same temperature for 1 h, the mixture was warmed to 0 ℃ and stirred for 20 minutes. Then, trimethyltin chloride (1 M, 26.4 mmol) was added to the mixture, and the mixture was warmed to room temperature. After stirring overnight, the mixture was quenched with water (20 mL) and extracted with petroleum ether (3 × 30 mL). The organic layer was dried with anhydrous $NaSO_4$. Crude **compound 2** (2.7 g, 43%) was obtained by removing the solvent. Compound 2 was not stable under ambient conditions and was immediately used for the next step reaction. ^{1}H NMR ($CDCl_3$, 400 MHz, δ/ppm): 7.47 (br, 1H), 7.06 (br, 1H), 5.06 (br, 2H), 3.48 (br, 3H), 0.52-0.14 (br, 9H). The broadening of the ^{1}H NMR spectrum could be caused by the easy oxidation of compound 2 and the generation of paramagnetic radical species. Due to the instability of compound 2, the ^{13}C NMR spectrum and MS were not acquired.

Compound 3. To a solution of dimethyl 2,3-dibromobut-2-enedicarboxylate (1.20 g, 3.97 mmol) and compound 2 (2.68 g, 8.73 mmol) in toluene (40 mL) was added $Pd(PPh_3)_4$ (459 mg, 0.40 mmol) and CuI (227 mg, 1.19 mmol) under nitrogen. The mixture was heated to reflux for 1 h. After cooling to room temperature, the mixture was poured into saturated aqueous NaCl and extracted with CH_2Cl_2 (3 × 40 mL). The combined organic layer was dried over anhydrous Na_2SO_4. After evaporation of the solvent, the residue was purified via column chromatography

(silica gel) by using CH_2Cl_2:ethyl acetate (40:1) as eluent to give **compound 3** as a yellow sticky oil (1.22 g, 72%). *Z* and *E* isomers (*Z*:*E* = 1:10) coexist in compound 3. Compound 3 was not stable (especially in solution) and was quickly used for the next step reaction. ^{1}H NMR ($CDCl_3$, 400 MHz, δ/ppm): 7.28 (d, *J* = 5.6 Hz, 2H, *E*), 7.24 (d, *J* = 5.6 Hz, 0.2H, *Z*), 6.91 (d, *J* = 5.6 Hz, 0.2H, *Z*), 6.86 (d, *J* = 5.6 Hz, 2H, *E*), 5.03 (s, 0.4H, *Z*), 5.00 (s, 4H, *E*), 3.81 (s, 6H, *E*), 3.70 (s, 0.6H, *Z*), 3.46 (s, 0.6H, *Z*), 3.40 (s, 6H, *E*). Due to the instability of compound 3, the ^{13}C NMR spectrum was not acquired. MALDI-TOF MS (m/z): $C_{18}H_{20}O_8S_2Na$ ($M + Na^+$) calc. 451.05, found 451.10.

Compound 4. To a solution of compound 3 (1.14 g, 2.66 mmol) in THF (19 mL) was added TMPMgCl·LiCl (1 M, 7.98 mmol) at -78 ℃ under nitrogen. After stirring at the same temperature for 2 h, 1,2-dibromotetrachloroethane (2.60 g, 7.98 mmol) was added to the mixture. Then the mixture was stirred for 20 minutes before being warmed to room temperature. After stirring for 30 minutes, the mixture was quenched with water and extracted with CH_2Cl_2. The organic layer was dried with anhydrous $NaSO_4$, filtered, and evaporated. The crude residue was purified via column chromatography (silica gel) by using CH_2Cl_2:ethyl acetate (40:1) as eluent to give the monobromination intermediate as a yellow solid (1.2 g). To the solution of the monobromination intermediate (1.16 g, 2.29 mmol) in THF (17 mL) was added TMPMgCl·LiCl (1 M, 5.73 mmol) at -78 ℃ under nitrogen. After stirring at the same temperature for 2 h, 1,2-dibromotetrachloroethane (1.87 g, 5.73 mmol) was added to the mixture. Then the mixture was stirred for 20 minutes before being warmed to room temperature. After stirring for 30 minutes, the mixture was quenched with water and extracted with CH_2Cl_2. The organic layer was dried with anhydrous $NaSO_4$, filtered, and evaporated. The crude residue was purified via column chromatography (silica gel) by using CH_2Cl_2:ethyl acetate (40:1) as eluent to give **compound 4** as a yellow solid (1.15 g, 74%). Compound 4 was not stable (especially in solution) and was quickly used for the next step reaction. ^{1}H NMR ($CDCl_3$, 400 MHz, δ/ppm): 6.92 (s, 2H), 4.97 (s, 4H), 3.80 (s, 6H), 3.40 (s, 6H). Due to the instability of compound 4, the ^{13}C NMR spectrum was not acquired. MALDI-TOF MS (m/z): $C_{18}H_{18}Br_2O_8S_2Na$ ($M + Na^+$). calc.606.87, found 606.89.

TPTP-Br. To a solution of compound 4 (1.15 g, 1.96 mmol) in toluene (19 mL) was added *p*-toluenesulfonic acid (34 mg, 0.2 mmol) under nitrogen. The mixture was stirred at 100 ℃ for 30 minutes and was poured into MeOH. The precipitate was collected and dried under vacuum to give **TPTP-Br** as an orange solid (655 mg, 77%). ^{1}H NMR ($CDCl_3$, 400 MHz, δ/ppm): 7.21 (s, 2H). The ^{13}C NMR spectrum and MS were not achievable due to the extremely low solubility of TPTP-Br.

Compound 5. To a solution of TPTP-Br (250 mg, 0.58 mmol) and tributyl(4-(2-butyloctyl)thiophen-2-yl)stannane (785 mg, 1.45 mmol) in toluene (5 mL) was added $Pd(PPh_3)_4$ (67 mg, 0.06 mmol) under nitrogen. The mixture was heated to reflux for 6 h and was poured into MeOH. The precipitate was collected and purified via column chromatography (silica gel) by using $CHCl_3$ as eluent to give **compound 5** as a brown solid (388 mg, 86%). ^{1}H NMR ($CDCl_3$, 400 MHz, δ/ppm): 7.19 (s, 2H), 7.13 (s, 2H), 6.92 (s, 2H), 2.53 (d, *J* = 6.8 Hz, 4H), 1.62 (m, 2H), 1.27-1.28 (m, 32H), 0.87-0.91 (m, 12H). ^{13}C NMR ($CDCl_3$, 100 MHz, δ/ppm):

158.96, 153.13, 143.73, 143.32, 135.46, 127.45, 122.87, 119.59, 111.99, 111.92, 38.84, 34.92, 33.28, 32.96, 31.89, 29.66, 28.83, 26.57, 23.03, 22.68, 14.14, 14.12. MALDI-TOF MS (m/z): $C_{52}H_{70}O_4S_4$ (M^+) calc. 776.31, found 776.29.

Compound 6. To a solution of TPTP-Br (250 mg, 0.58 mmol) and tributyl(4-(2-hexyldecyl)thiophen-2-yl)stannane (867 mg, 1.45 mmol) in toluene (5 mL) was added $Pd(PPh_3)_4$ (67 mg, 0.06 mmol) under nitrogen. The mixture was heated to reflux for 6 h and was poured into MeOH. The precipitate was collected and purified via column chromatography (silica gel) by using $CHCl_3$ as eluent to give **compound 6** as a brown solid (434 mg, 85%). ^{1}H NMR ($CDCl_3$, 400 MHz, δ/ppm): 7.17 (s, 2H), 7.12 (s, 2H), 6.91 (s, 2H), 2.52 (d, *J* = 6.8 Hz, 4H), 1.61 (m, 2H), 1.27 (m, 48H), 0.86-0.90 (m, 12H). ^{13}C NMR ($CDCl_3$, 100 MHz, δ/ppm): 158.92, 153.11, 143.73, 143.30, 135.45, 127.43, 122.85, 119.54, 111.95, 111.89, 38.87, 34.93, 33.27, 31.91, 31.89, 29.99, 29.67, 29.63, 29.33, 26.59, 26.56, 22.68, 14.12. MALDI-TOF MS (m/z): $C_{52}H_{72}O_4S_4$ (M^+) calc. 888.43, found 888.46.

Compound 7. To a solution of compound 5 (308 mg, 0.40 mmol) in $CHCl_3$ (44 mL) and DMF (2.5 mL) was added NBS (157 mg, 0.88 mmol) at room temperature. The mixture was stirred for 13 h. The mixture passed through a short silica gel column ($CHCl_3$ as eluent). Then, the solution was poured into MeOH. The precipitate was collected and dried under vacuum to give **compound 7** as a brown solid (367 mg, 98%). ^{1}H NMR ($CDCl_3$, 400 MHz, δ/ppm): 7.10 (s, 2H), 7.06 (s, 2H), 2.50 (d, *J* = 7.2 Hz, 4H), 1.68 (m, 2H), 1.27-1.29 (m, 32H), 0.86-0.92 (m, 12H). ^{13}C NMR ($CDCl_3$, 100 MHz, δ/ppm): 158.68, 153.10, 143.13, 142.17, 135.12, 126.83, 119.53, 112.09, 112.05, 111.93, 38.54, 34.22, 33.31, 33.01, 31.89, 29.67, 28.74, 26.49, 23.04, 22.68, 14.13. Single crystals of compound 7 were obtained via slow vapor diffusion of hexane into its $CHCl_3$ solution. Formula: $C_{44}H_{54}Br_2O_4S_4$; formula weight: 934.93; crystal system: triclinic; space group: *P* -1; color of crystal: dark brown; unit cell parameters: a = 7.652(3) Å, b = 8.553(3) Å, c = 18.197(7) Å, α = 92.808(13)°, β = 94.579(13)°, γ = 109.208(11)°, V = 1117.47(7) Å^3; temperature for data collection: 170.00(10) K; *Z* = 1; final *R* indices [I >2σ(I)]: *R1* = 0.0810, *wR2* = 0.2915; GOF on F^2: 1.002. The crystallographic data have been deposited in Cambridge Crystallographic Data Centre (**CCDC-2167880**). MALDI-TOF MS (m/z): $C_{44}H_{54}Br_2O_4S_4$ (M^+) calc. 932.13, found 932.15.

Compound 8. To a solution of compound 7 (400 mg, 0.45 mmol) in $CHCl_3$ (26 mL) and DMF (5 mL) was added NBS (176 mg, 0.99 mmol) at room temperature. The mixture was stirred for 13 h. The mixture passed through a short silica gel column ($CHCl_3$ as eluent). Then, the solution was poured into MeOH. The precipitate was collected and dried under vacuum to give **compound 8** as a brown solid (462 mg, 98%). ^{1}H NMR ($CDCl_3$, 400 MHz, δ/ppm): 7.10 (s, 2H), 7.05 (s, 2H), 2.49 (d, *J* = 7.1 Hz, 4H), 1.68 (m, 2H), 1.27 (m, 48H), 0.85-0.90 (m, 12H). ^{13}C NMR ($CDCl_3$, 100 MHz, δ/ppm): 158.65, 153.10, 143.13, 142.18, 135.11, 126.83, 119.49, 112.05, 111.94, 38.56, 34.23, 33.33, 31.91, 31.89, 29.99, 29.67, 29.62, 29.34, 26.53, 26.49, 22.68, 14.13. MALDI-TOF MS (m/z): $C_{52}H_{70}Br_2O_4S_4$ (M^+) calc. 1044.25, found 1044.27.

PBDTTPTP. To a mixture of compound 8 (150 mg, 0.14 mmol), BDT-Si-Sn (141.8 mg, 0.14 mmol), $Pd_2(dba)_3$ (3.9 mg, 0.0043 mmol) and P(o-Tol)$_3$ (13.1 mg, 0.043 mmol) in a Schlenk

flask was added toluene (2.9 mL) under argon. The mixture was heated to reflux for 17 h. Then the solution was cooled to room temperature and added into 150 mL methanol dropwise. The precipitate was collected and further purified via Soxhlet extraction by using $CHCl_3$ and chlorobenzene in sequence. The chlorobenzene fraction was concentrated and added into methanol dropwise. The precipitate was collected and dried under vacuum overnight to give **PBDTTPTP** as a brown solid (148 mg, 67%). The M_n for PBDTTPTP is 51.6 kDa, with a PDI of 1.80. ^{1}H NMR ($CDCl_3$, 400 z, δ/ppm): 6.45-6.84 (br, aromatic protons), 2.90 (br, aliphatic protons), 0.67-1.54 (br, aliphatic protons).

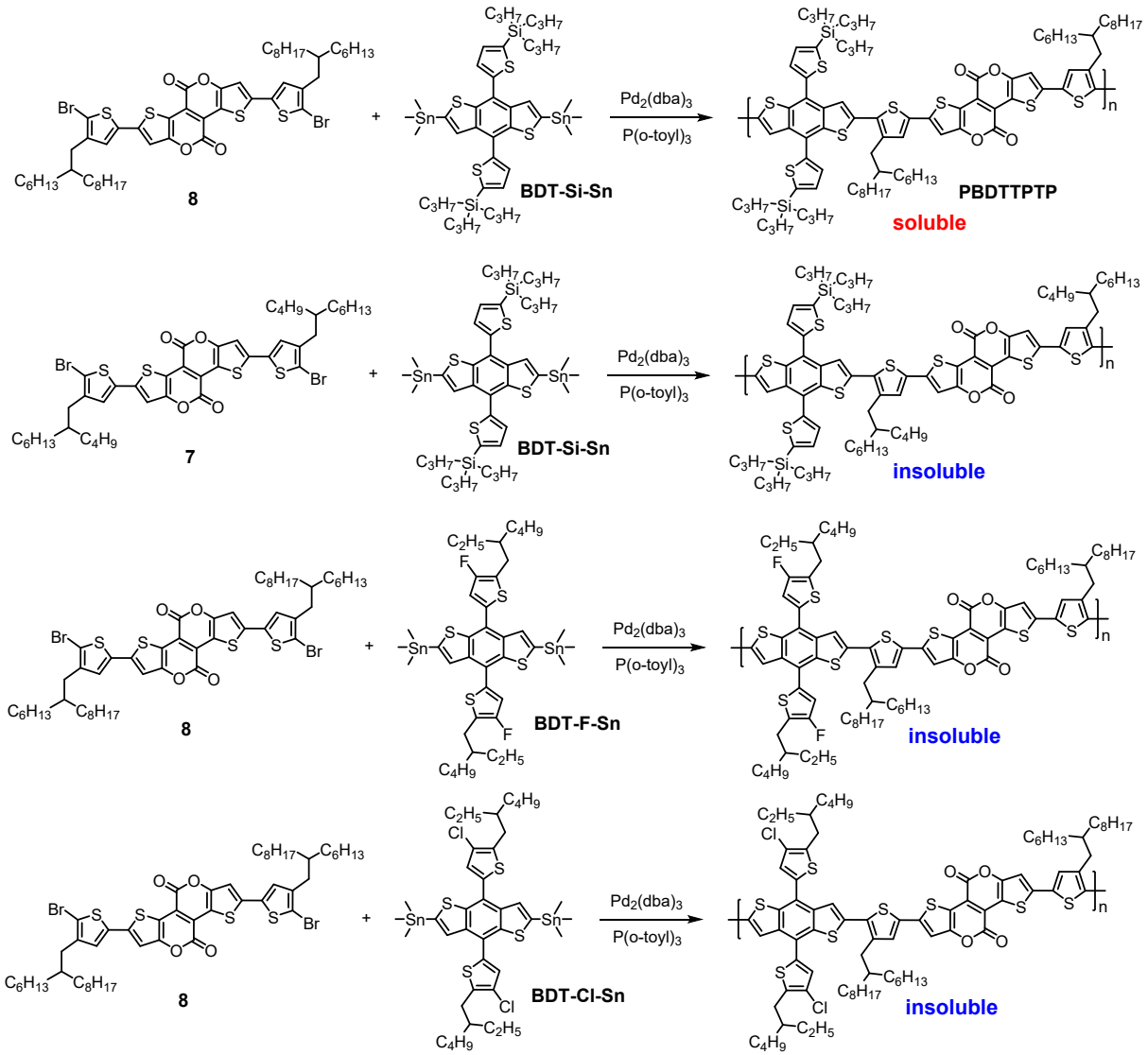

Scheme S1 The attempts of copolymerization.

3. NMR

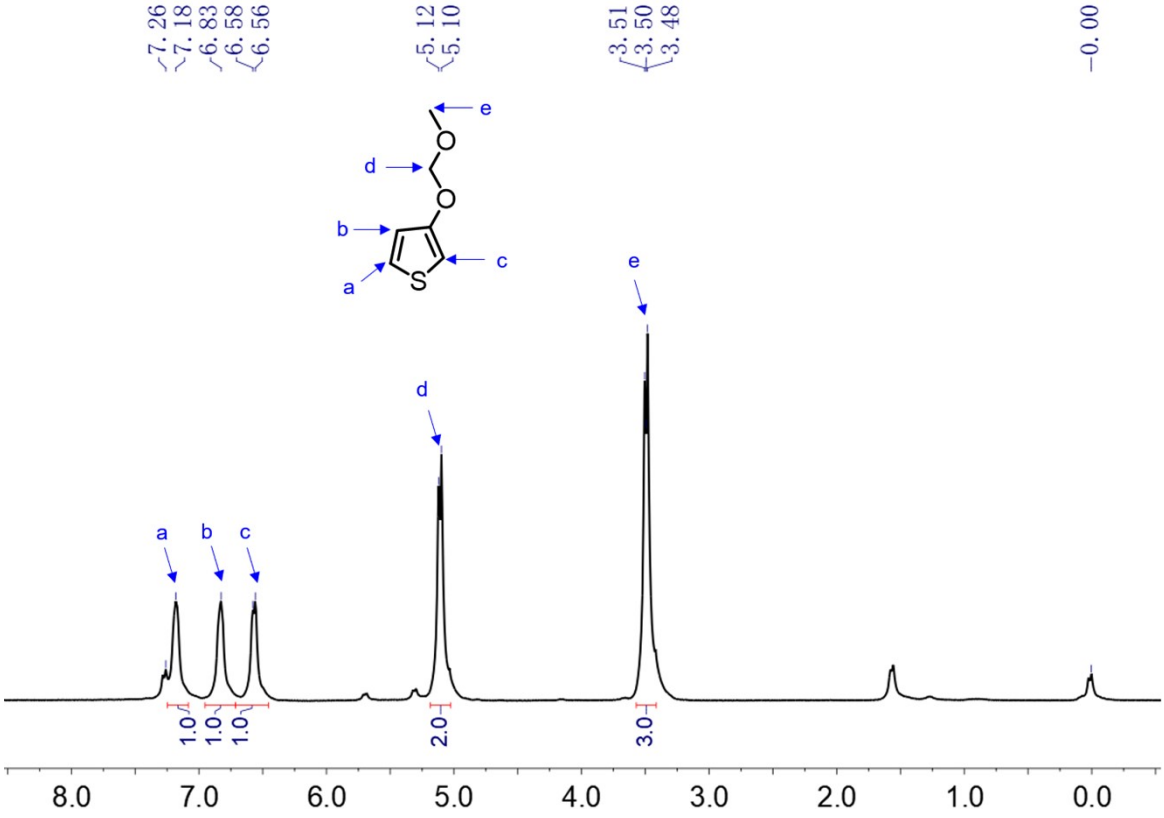

Fig. S1 [1]H NMR spectrum of **compound 1**.

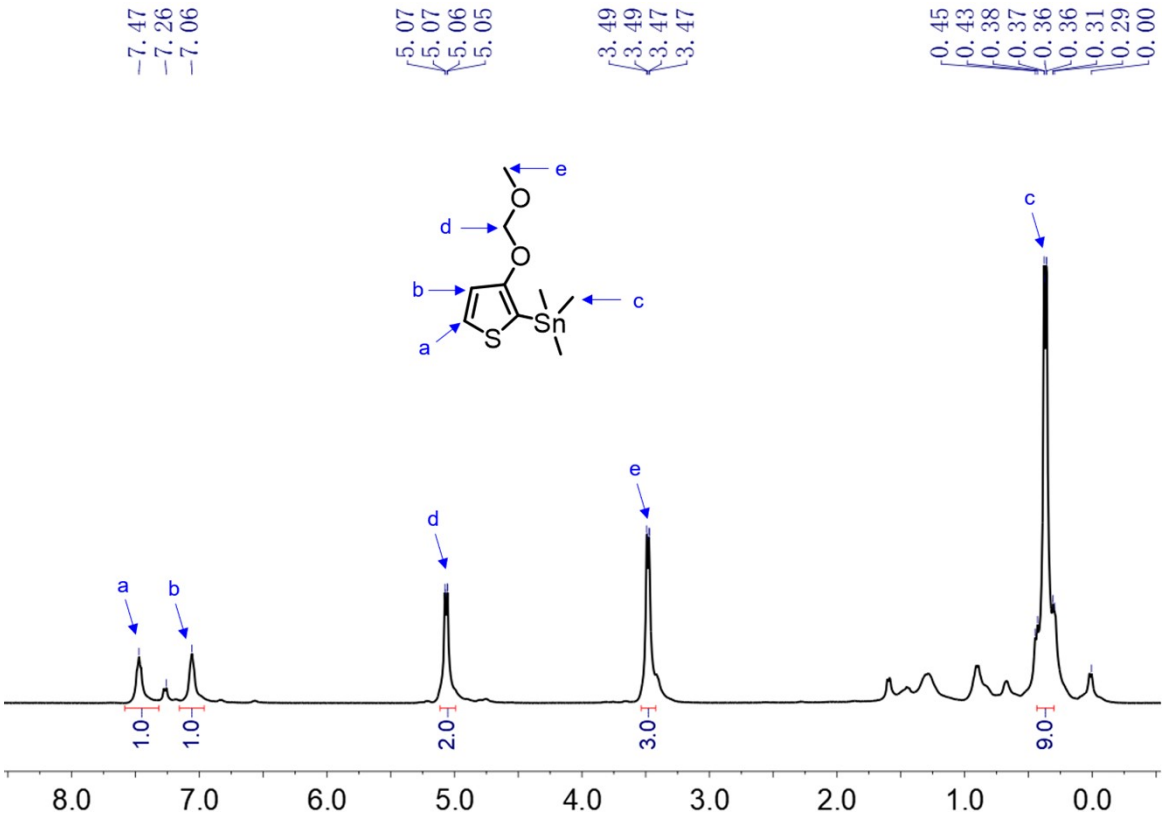

Fig. S2 [1]H NMR spectrum of **compound 2**.

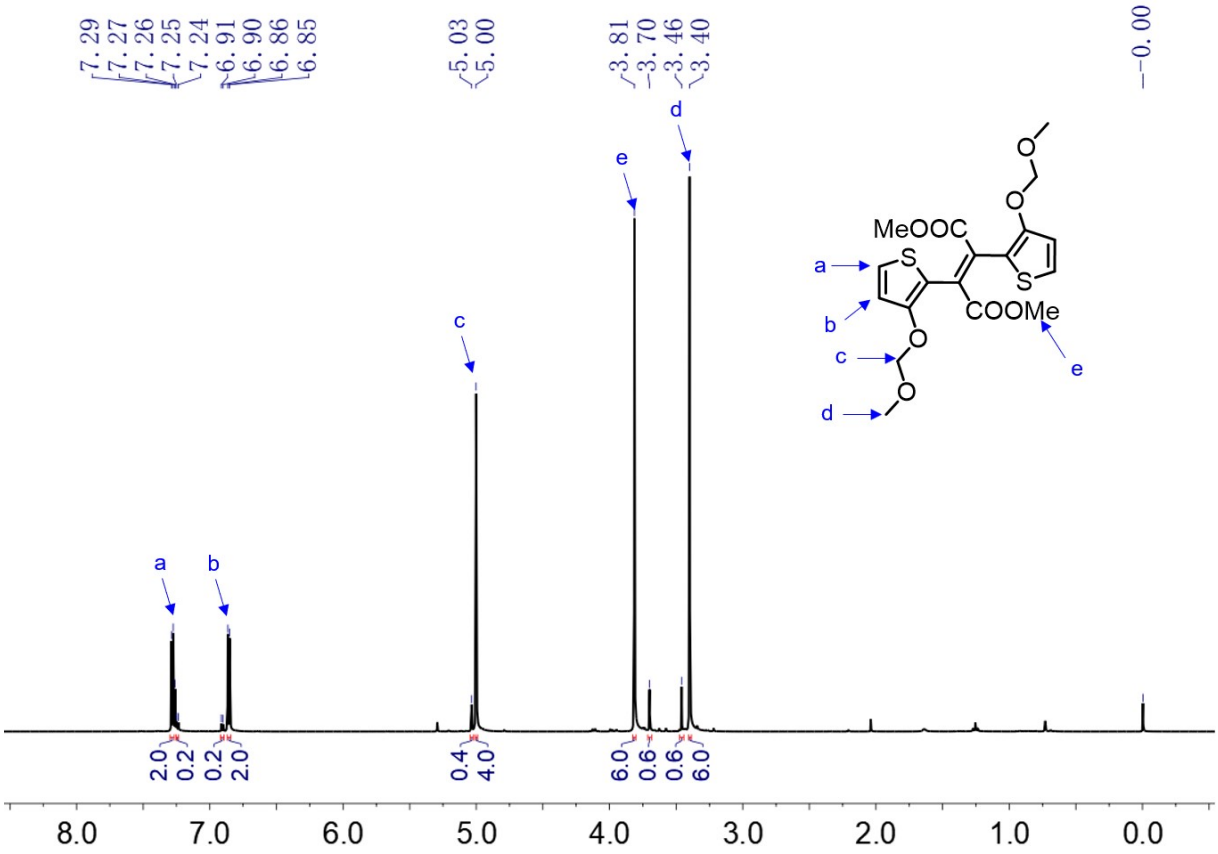

Fig. S3 ^{1}H NMR spectrum of **compound 3**.

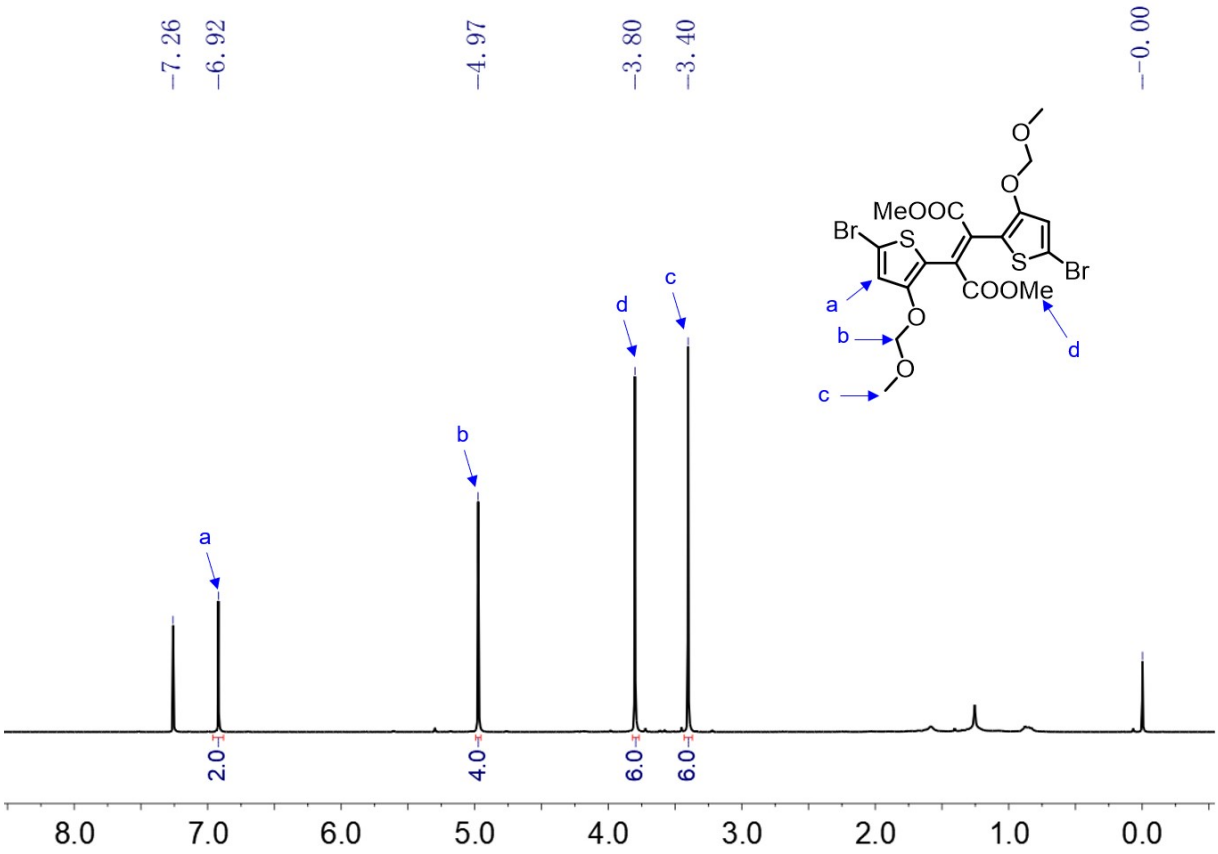

Fig. S4 ^{1}H NMR spectrum of **compound 4**.

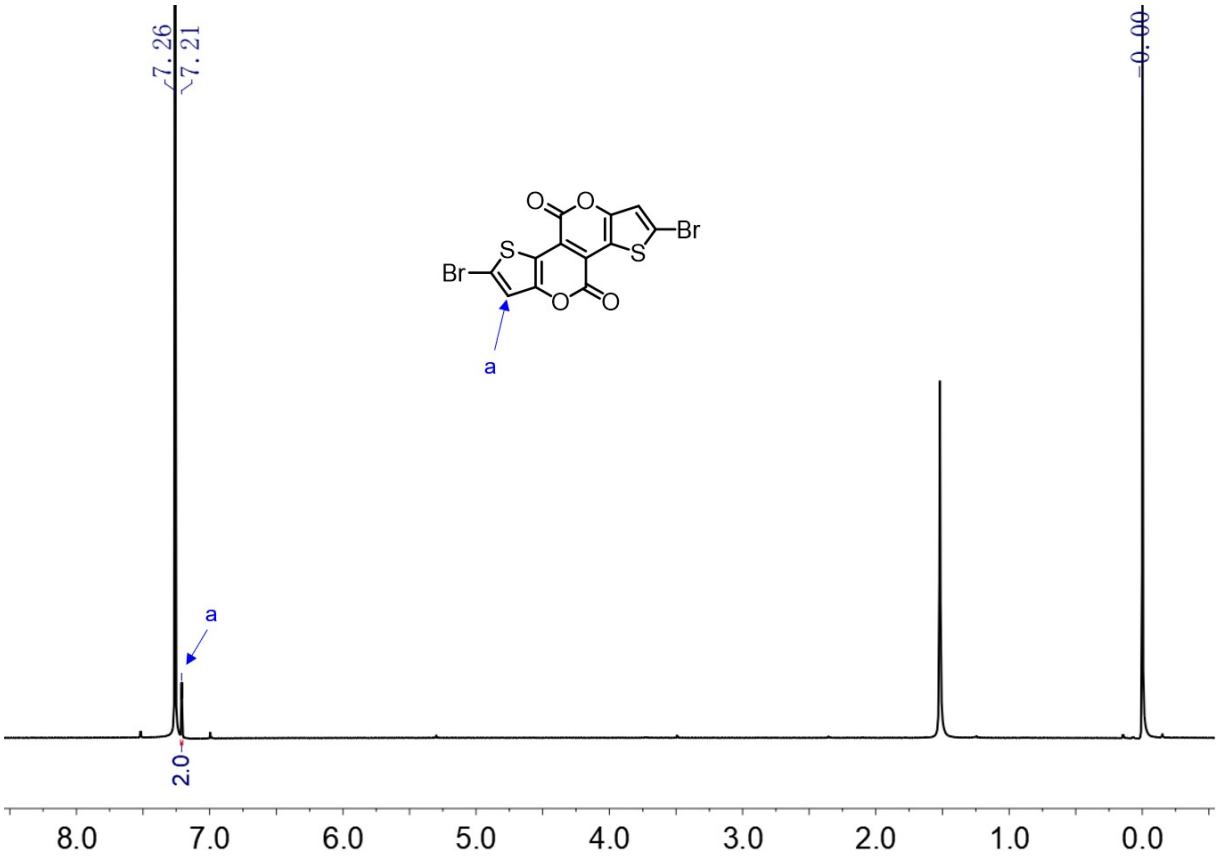

Fig. S5 ^{1}H NMR spectrum of **TPTP-Br**.

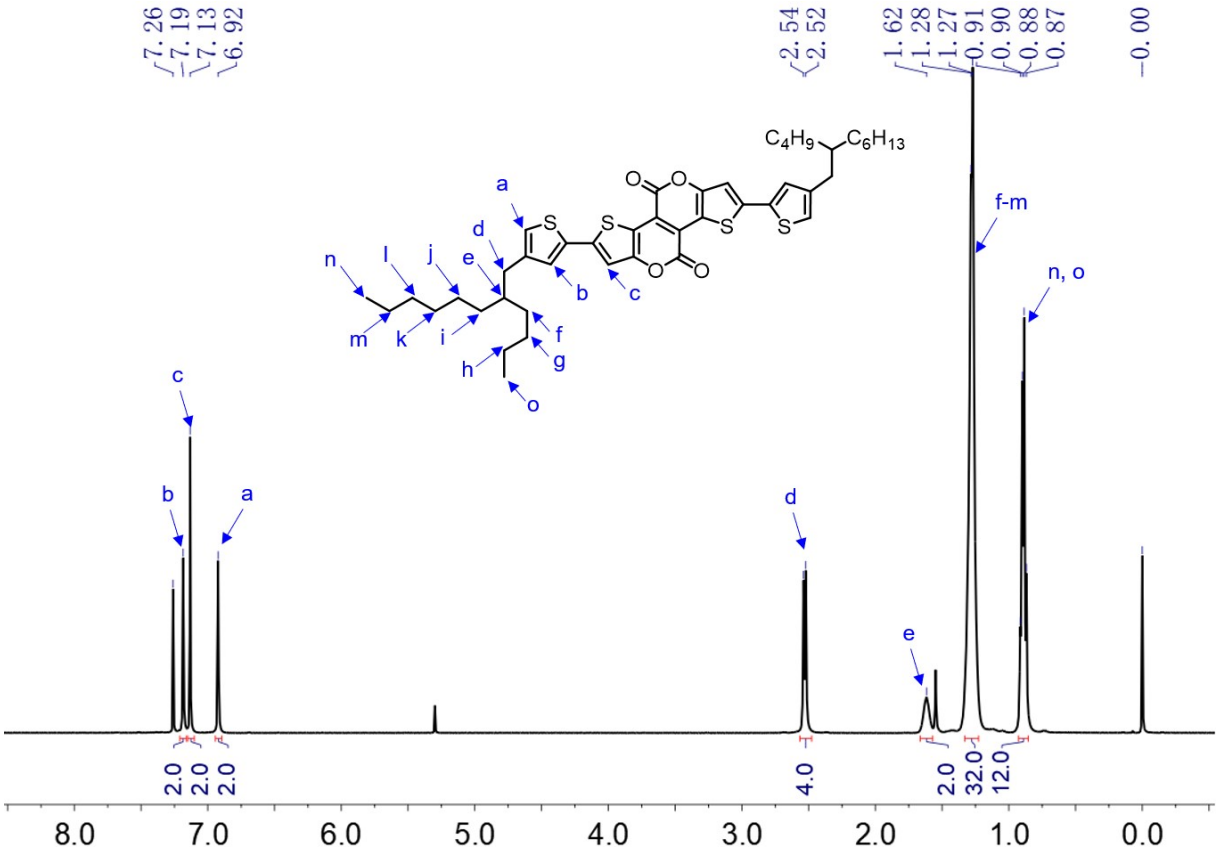

Fig. S6 ^{1}H NMR spectrum of **compound 5**

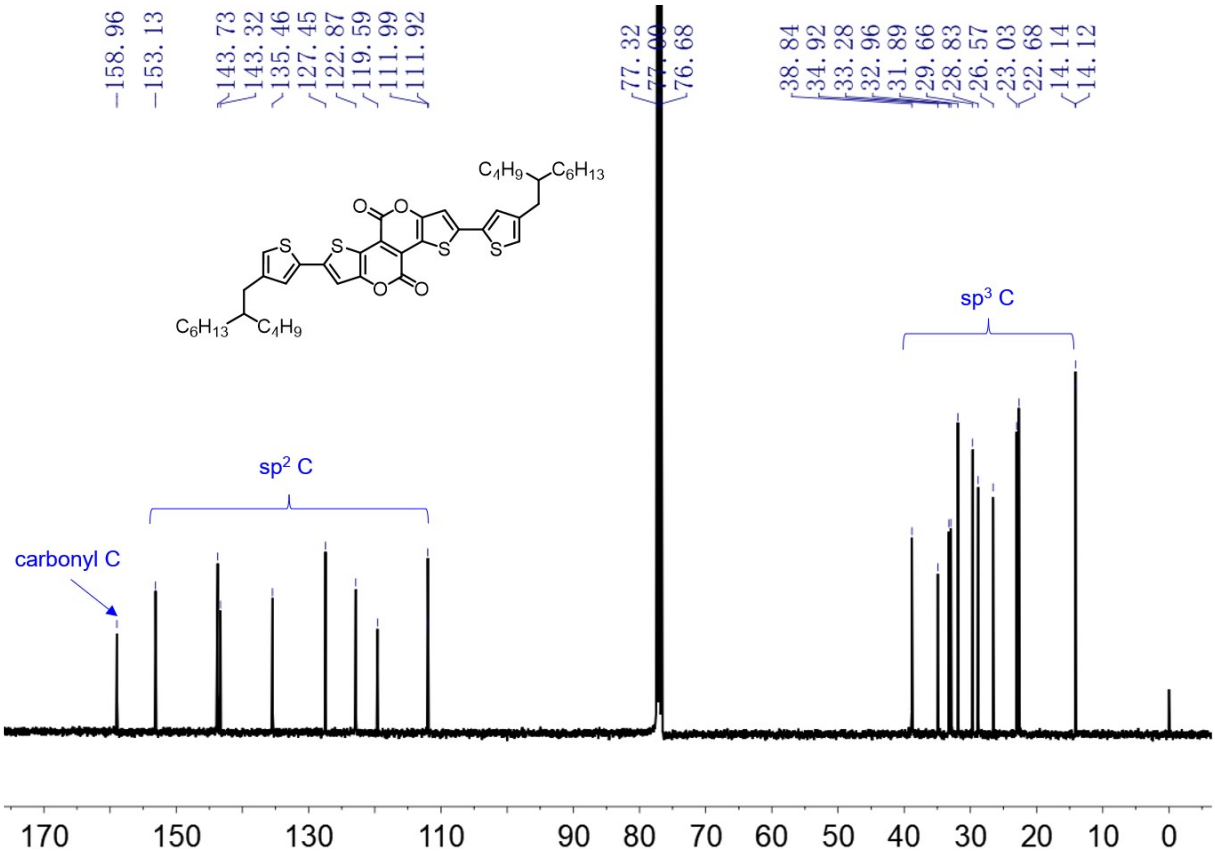

Fig. S7 ^{13}C NMR spectrum of **compound 5**.

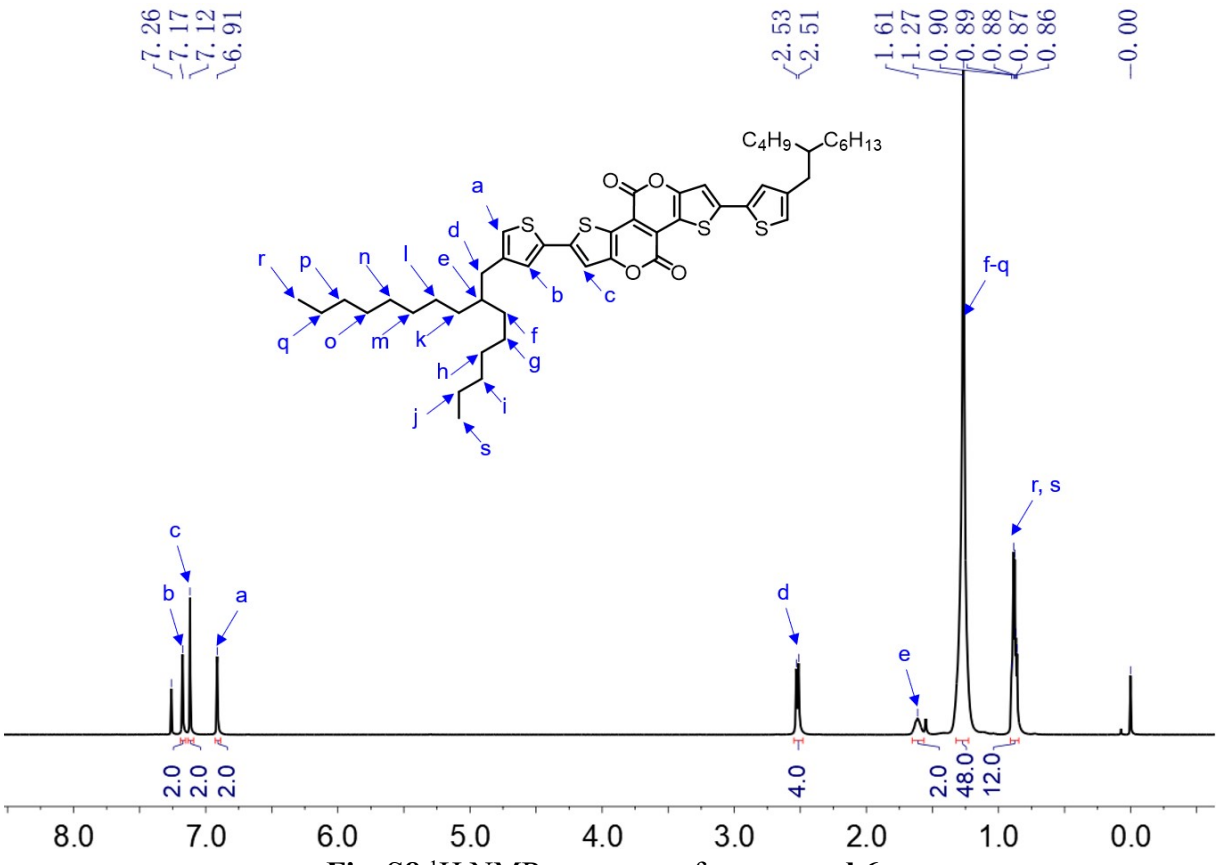

Fig. S8 ^{1}H NMR spectrum of **compound 6**.

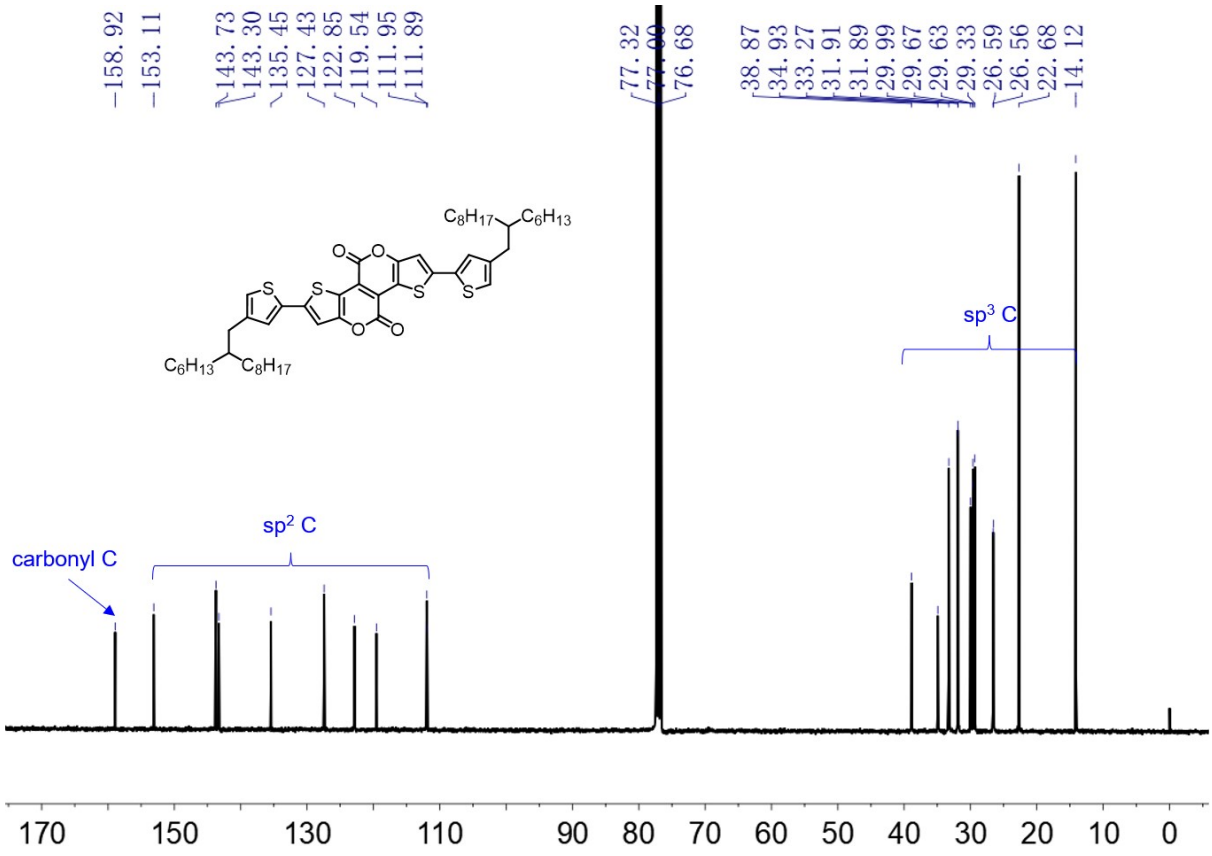

Fig. S9 ^{13}C NMR spectrum of **compound 6**.

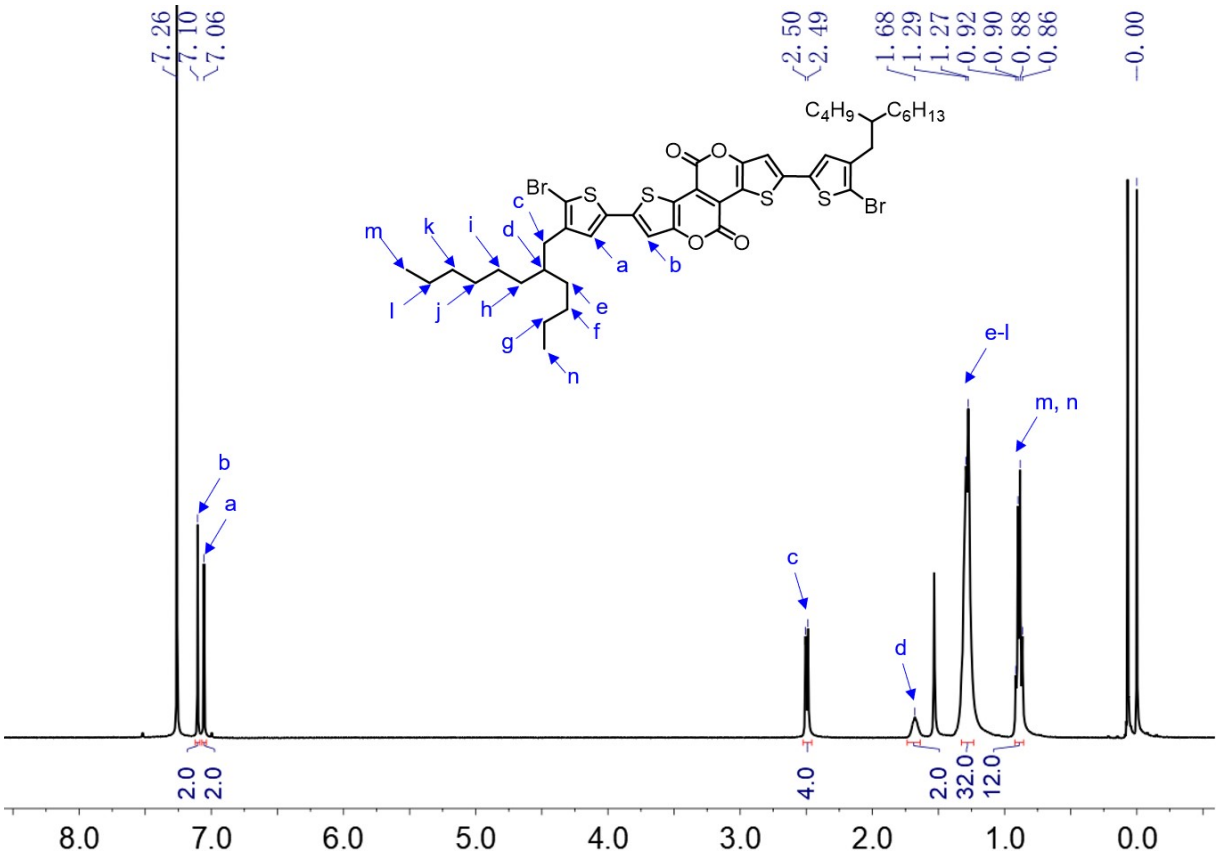

Fig. S10 ^{1}H NMR spectrum of **compound 7**.

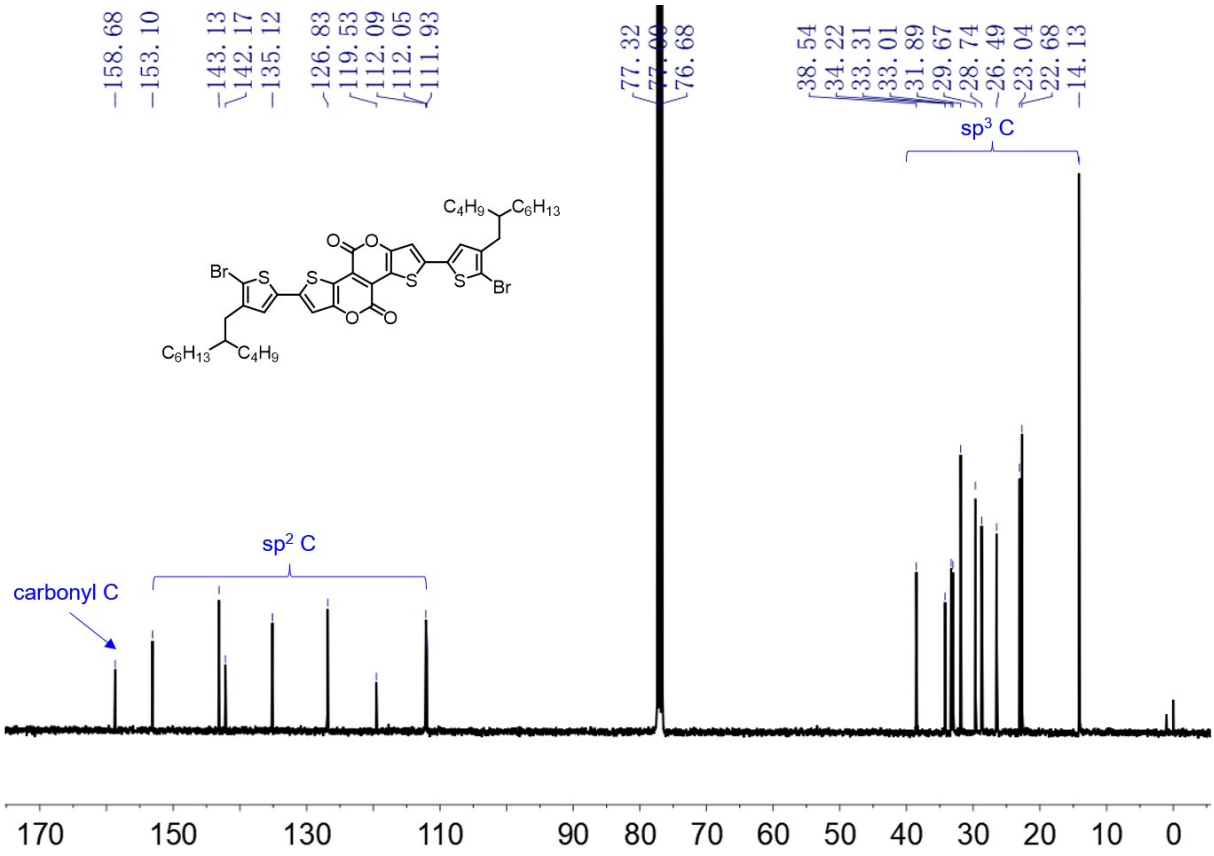

Fig. S11 ^{13}C NMR spectrum of **compound 7**.

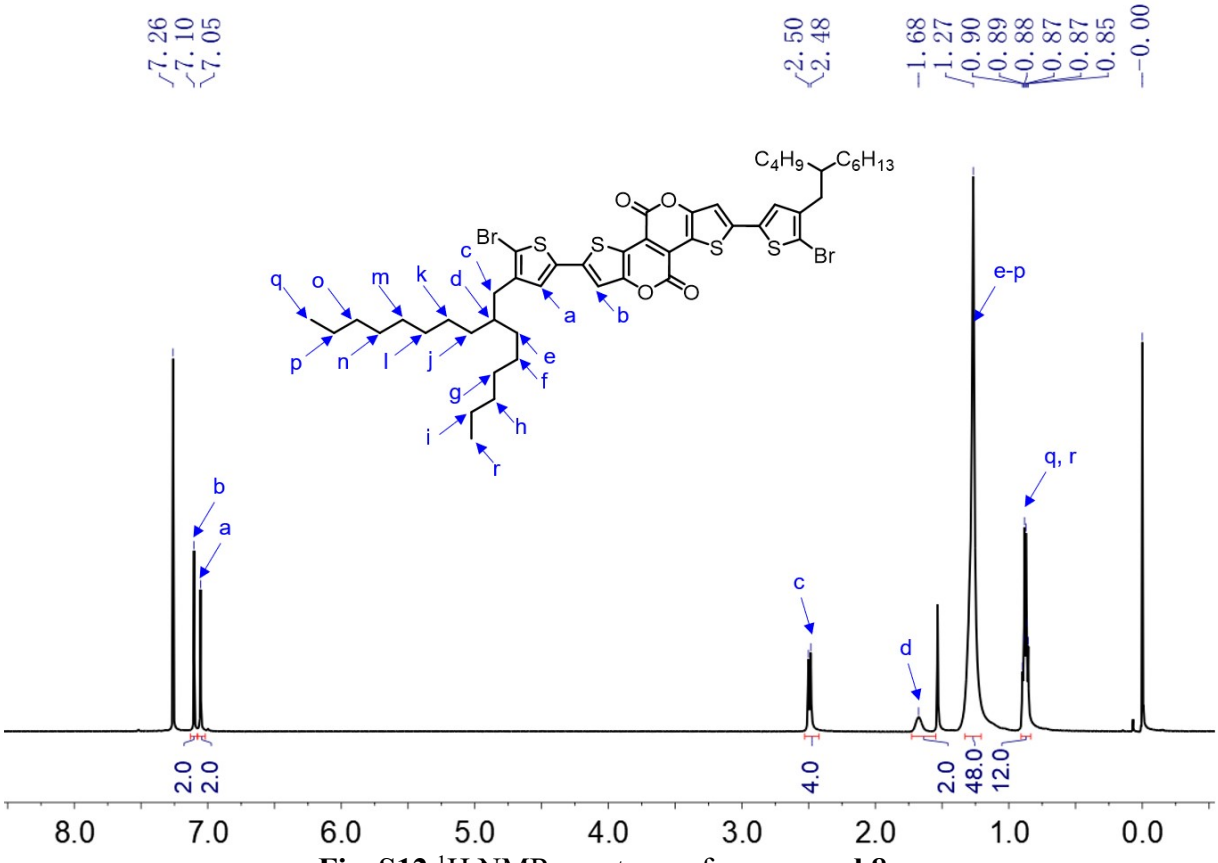

Fig. S12 ^{1}H NMR spectrum of **compound 8**.

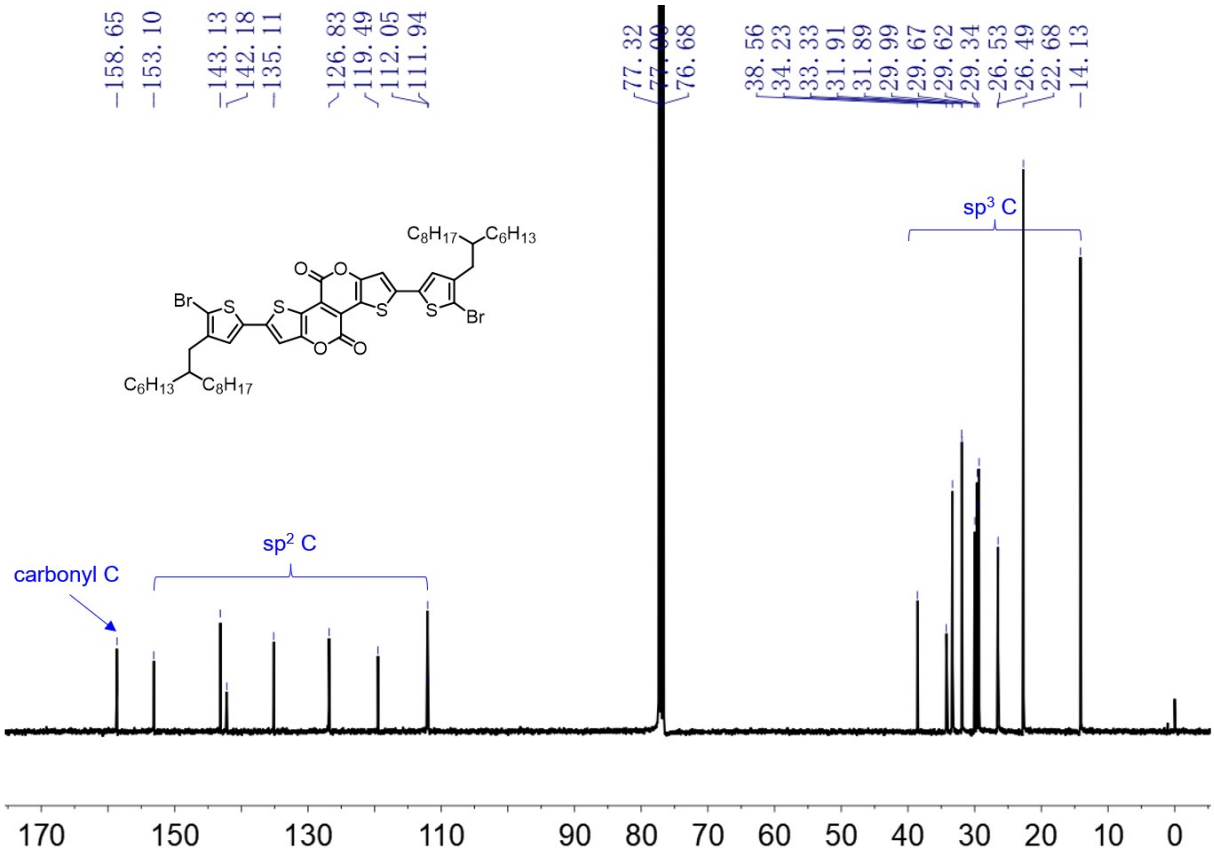

Fig. S13 ^{13}C NMR spectrum of **compound 8**.

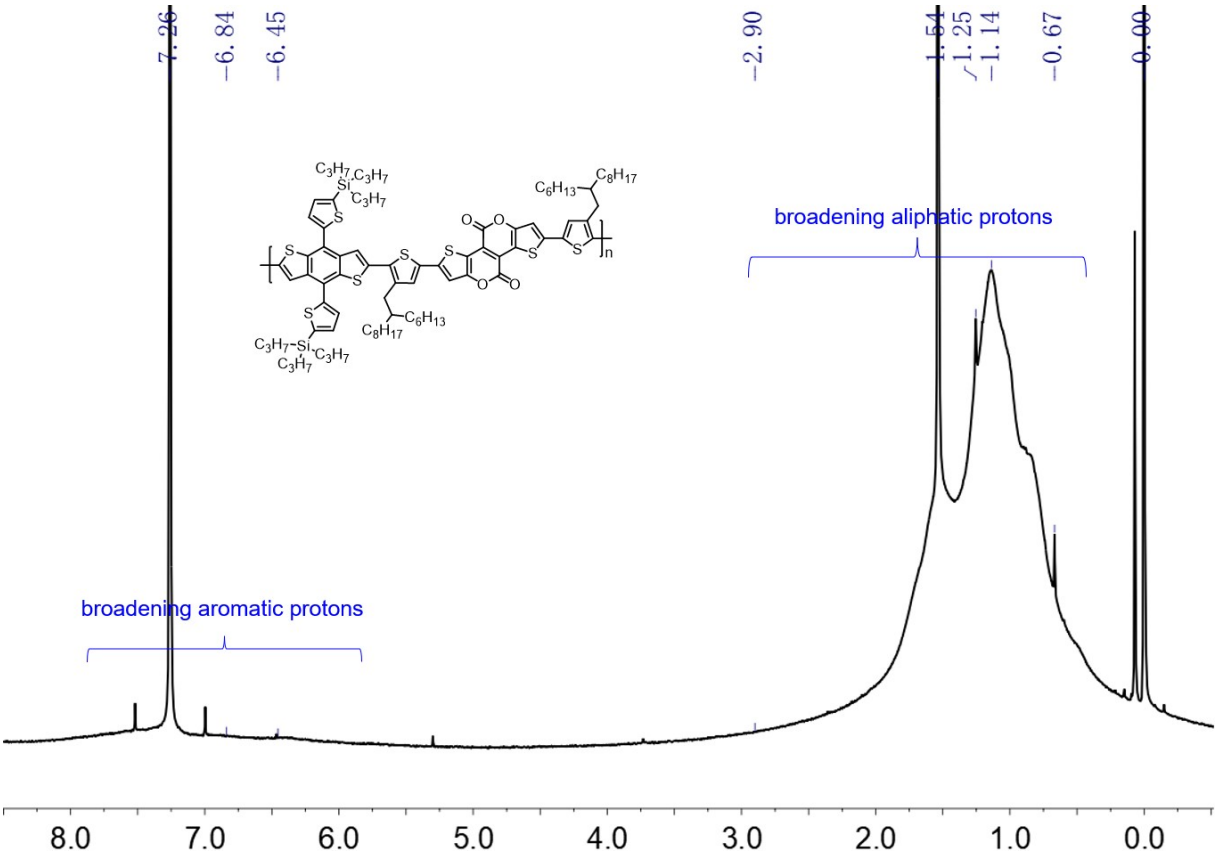

Fig. S14 ^{1}H NMR spectrum of **PBDTTPTP**.

4. Synthetic complexity analysis

The synthetic complexity (SC) was calculated with following equation. [4,5]

$$SC = 35\frac{NSS}{NSS_{max}} + 25\frac{\log RY}{\log RY_{max}} + 15\frac{NUO}{NUO_{max}} + 15\frac{NCC}{NCC_{max}} + 10\frac{NHC}{NHC_{max}}$$

Where NSS is the number of synthetic steps, RY is the reciprocity yields, NUO is the number of unit operations, NCC is the number of column chromatography, and NHC is the number of hazardous chemicals used for their preparation. The values of NSS_{max}, RY_{max}, NUO_{max}, NCC_{max} and NHC_{max} used for the normalization of the parameters are the maximum values selected in each set.

Table S1 The calculated SC for the polymers in Fig. 1.

Polymer	NSS	RY [a]	NUO	NCC	NHC [b]	SC (%) [c]
PBDTT-DPP [5]	10	6	16	3	31	46.16
PIDT-PhanQ [5]	14	6.9	23	7	39	64.67
PCPDTFBT [5]	14	13.6	33	12	29	78.36
PDTP-DFBT [5]	14	14.5	28	11	31	75.40
PTB7-Th [5]	16	15	24	7	31	73.15
PM6	13	80	20	7	102	81.28
PBDTTPTP	11	13.8	21	8	85	66.91

[a] RY = Σ (100/yield of the comonomers) %

[b] Chemicals are counted as many times as the number of their H risk phrases (according to CE Regulation n. 1272/2008)

[c] NSS_{max} = 16, RY_{max} = 80, NUO_{max} = 33, NCC_{max} = 12, NHC_{max} = 102.

5. Device fabrication and measurements

Conventional solar cells

A 30 nm thick PEDOT:PSS (CLEVIOSTM P VP Al 4083 from Heraeus) layer was made by spin-coating an aqueous dispersion onto ITO glass (4000 rpm for 25 s). PEDOT:PSS substrates were dried at 150 °C for 15 min. An active blend solution (PBDTTPTP:N3 in CF) was spin-coated onto PEDOT:PSS. PDIN (2 mg/mL, Organtec Co.) in MeOH:AcOH (1000:3) was spin-coated onto active layer (5000 rpm for 30 s). Ag (~80 nm) was evaporated onto PDIN through a shadow mask (pressure ca. 10^{-4} Pa). The effective area for the devices is 4 mm^2. The thicknesses of the active layers were measured by using a KLA Tencor D-120 profilometer. *J-V* curves were measured by using a computerized Keithley 2400 SourceMeter and a Xenon-lamp-based solar simulator (Enli Tech, AM 1.5G, 100 mW/cm^2). The illumination intensity of solar simulator was determined by using a monocrystalline silicon solar cell (Enli SRC2020, 2cm×2cm) calibrated by the National Institute of Metrology (NIM). The external quantum efficiency (EQE) spectra were measured by using a QE-R3011 measurement system (Enli Tech).

Semitransparent solar cells

A 30 nm thick PEDOT:PSS layer was made by spin-coating an aqueous dispersion onto ITO glass (4000 rpm for 25 s). PEDOT:PSS substrates were dried at 150 °C for 15 min. An active blend solution (PBDTTPTP:N3 in CF) with different ratio was spin-coated onto PEDOT:PSS. PDIN (2 mg/mL) in MeOH:AcOH (1000:3) was spin-coated onto active layer (5000 rpm for 30 s). Au (0, 1, 1.5 nm) was evaporated onto PDIN through a shadow mask (pressure ca. 10^{-4} Pa). Then, Ag (10, 15, 20, 30 nm) was evaporated onto Au through a shadow mask (pressure ca. 10^{-4} Pa). MgF_2 (~100 nm) was evaporated onto glass and MoO_3 (~35 nm) was evaporated onto Ag as ARC.

Hole-only devices

The structure for hole-only devices is ITO/PEDOT:PSS/active layer/MoO_3/Al. A 30 nm thick PEDOT:PSS layer was made by spin-coating an aqueous dispersion onto ITO glass (4000 rpm for 25 s). PEDOT:PSS substrates were dried at 150 °C for 10 min. Pure donor or an active blend in CF was spin-coated onto PEDOT:PSS layer. Finally, MoO_3 (~6 nm) and Al (~100 nm) was successively evaporated onto the active layer through a shadow mask (pressure ca. 10^{-4} Pa). *J-V* curves were measured by using a computerized Keithley 2400 SourceMeter in the dark.

Electron-only devices

The structure for electron-only devices is ITO/ZnO/active layer/Al. The ZnO precursor solution was spin-coated onto ITO glass (4000 rpm for 30 s). The films were annealed at 200 °C in air for 20 min. An active blend in CF was spin-coated onto ZnO. Al (~100 nm) was successively evaporated onto the active layer through a shadow mask (pressure ca. 10^{-4} Pa). *J*-V curves were measured by using a computerized Keithley 2400 SourceMeter in the dark.

6. SCLC measurements for pure PBDTTPTP film

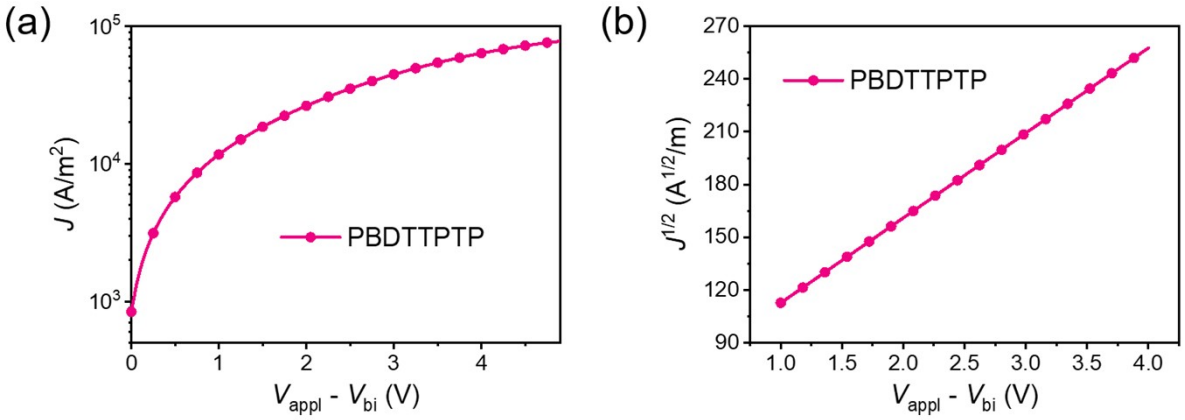

Fig. S15. *J-V* curve (a) and corresponding $J^{1/2}$-*V* plot (b) for the hole-only device (in dark). The thickness for PBDTTPTP film is 94 nm.

7. CV

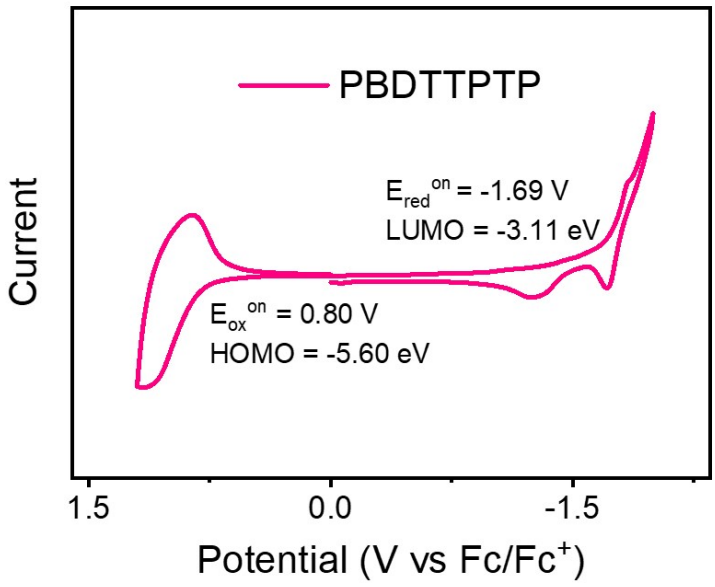

Fig. S16 Cyclic voltammogram for PBDTTPTP

8. AVT

The average visible light transmittance (AVT) [6] are calculated according to the equation:

$$AVT = \frac{\int T(\lambda) \times V(\lambda) \times AM1.5Gd(\lambda)}{\int V(\lambda) \times AM1.5Gd(\lambda)}$$

Where $T(\lambda)$ is the transmission spectrum, $V(\lambda)$ is the photopic response of human eye, $AM1.5G(\lambda)$ is photon flux. It is estimated by taking the average of the transparency of the devices in the visible region (380-740 nm) based on the photonic response of the human eye.

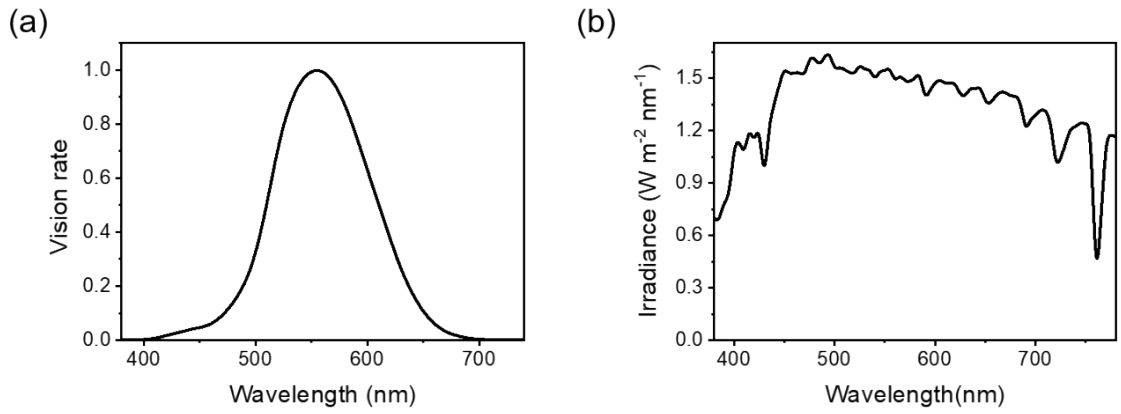

Fig. S17 (a) The photopic response of human eye $V(\lambda)$ and (b) photon flux of $AM1.5G(\lambda)$.

9. Optimization of the active layer thickness for PBDTTPTP:N3 opaque solar cells

Table S2 Optimization of the active layer thickness for PBDTTPTP:N3 opaque solar cells.[a]

Thickness [nm]	V_{oc} [V]	J_{sc} [mA/cm^2]	FF [%]	PCE [%]
160	0.822	24.93	71.1	14.56 (14.42)[b]
128	0.829	25.43	72.5	15.28 (15.17)
119	0.828	25.23	72.6	15.16 (15.07)
102	0.826	25.30	71.7	14.98 (14.91)
88	0.822	25.19	70.8	14.66 (14.31)

[a]D/A ratio: 1:1.4 (w/w); blend solution: 12 mg/mL in CF.
[b]Data in parentheses stand for the average PCEs for 10 cells.

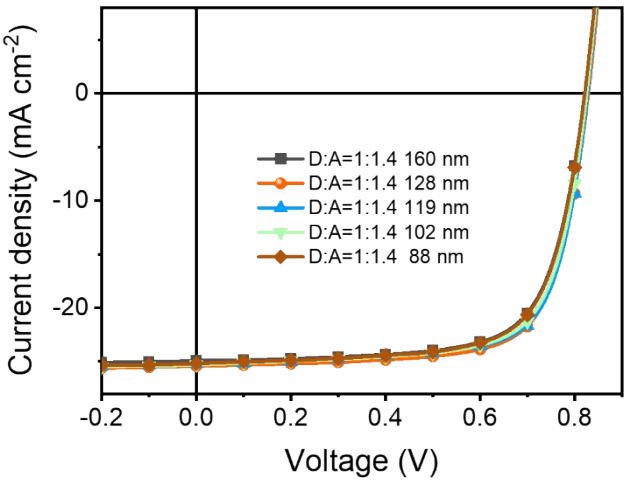

Fig. S18 *J*-V curves for PBDTTPTP:N3 opaque solar cells with different active layer thickness.

10. SCLC measurements for blend films.

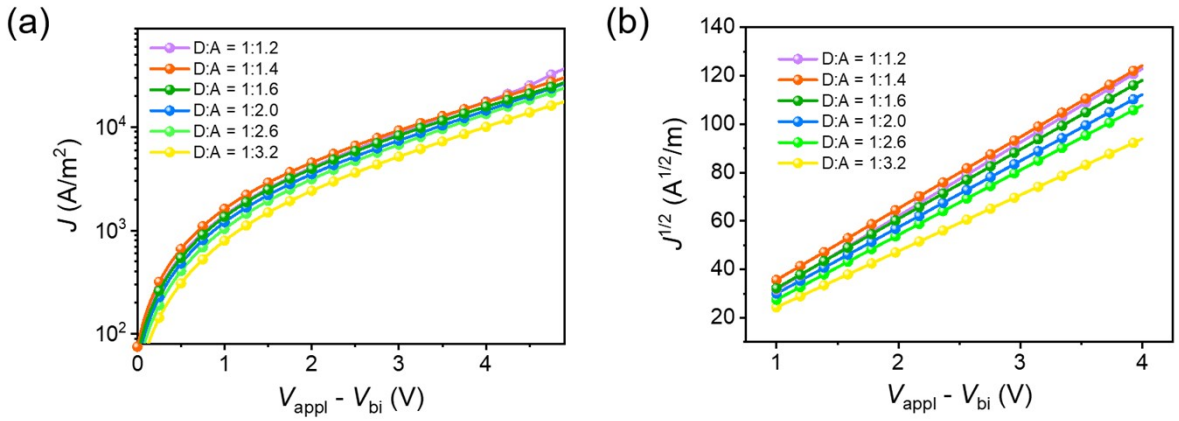

Fig. S19 *J-V* curves (a) and corresponding $J^{1/2}$-*V* plots (b) for the hole-only devices (in dark). The thicknesses for D:A ratio of 1:1.2, 1:1.4, 1:1.6, 1:2.0, 1:2.6 and 1:3.2 blend films are 130 nm, 132 nm, 133 nm,136 nm, 138 nm and 149 nm, respectively.

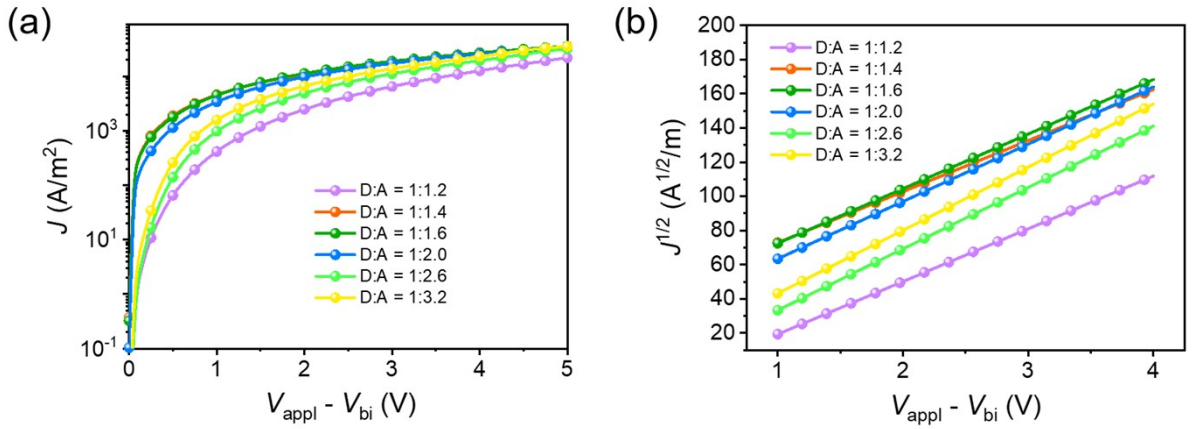

Fig. S20 *J-V* curves (a) and corresponding $J^{1/2}$-*V* plots (b) for the electron-only devices (in dark). The thicknesses for D:A ratio of 1:1.2, 1:1.4, 1:1.6, 1:2.0, 1:2.6 and 1:3.2 blend films are 113 nm, 115 nm, 112 nm, 111 nm, 108 nm and 106 nm, respectively.

Table S3 Hole and electron mobilities.

D:A [w:w]	μ_h [cm^2/Vs]	μ_e [cm^2/Vs]
1:1.2	6.80×10^{-4}	4.46×10^{-4}
1:1.4	6.70×10^{-4}	5.23×10^{-4}
1:1.6	6.45×10^{-4}	5.41×10^{-4}
1:2.0	6.32×10^{-4}	5.47×10^{-4}
1:2.6	6.29×10^{-4}	5.60×10^{-4}
1:3.2	5.94×10^{-4}	5.85×10^{-4}

11. AFM

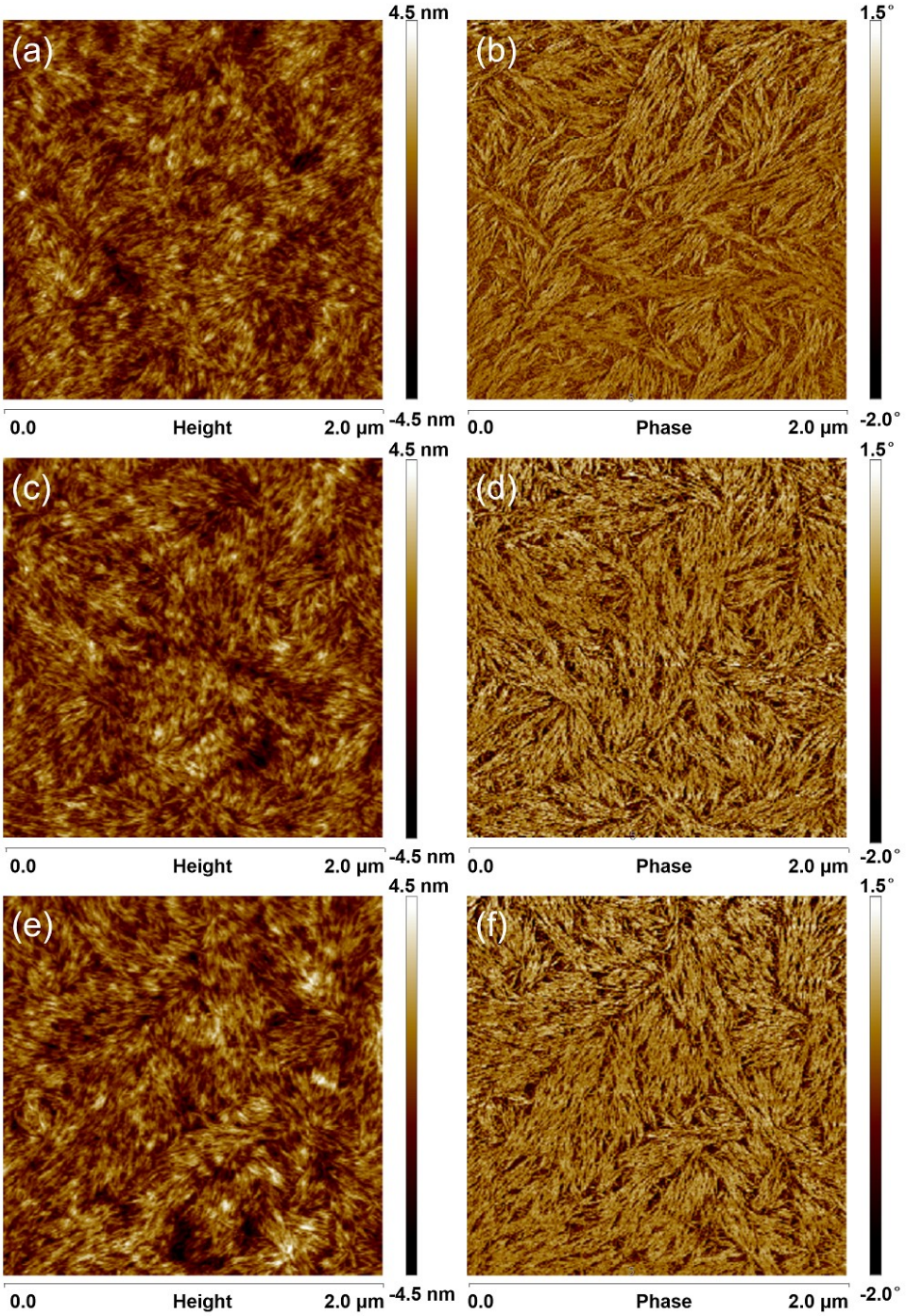

Fig. S21 AFM height (left) images and phase (right) images for the typical blend films. (a, b) PBDTTPTP:N3 = 1:1.4, (c, d) PBDTTPTP :N3 = 1:2.0 and (e, f) PBDTTPTP :N3 = 1:2.6.

12. Charge recombination analysis

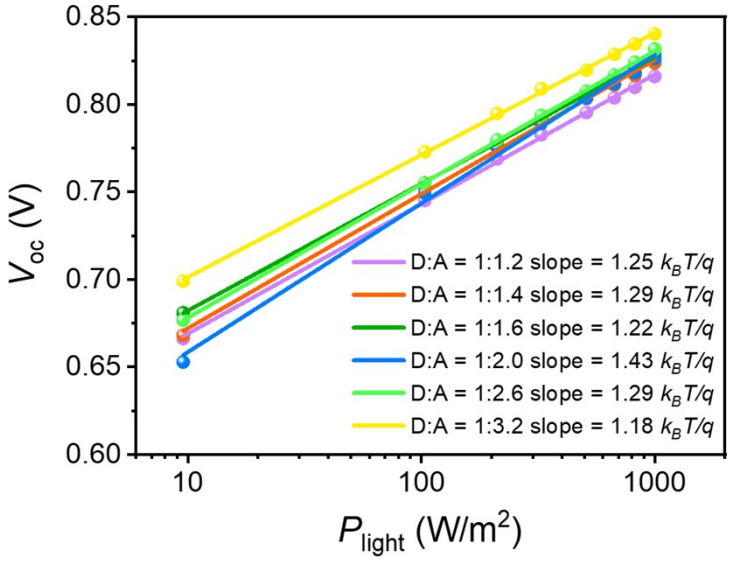

Fig. S22 V_{oc}-P_{light} plots for the PBDTTPTP:N3 solar cells with different D/A ratios.

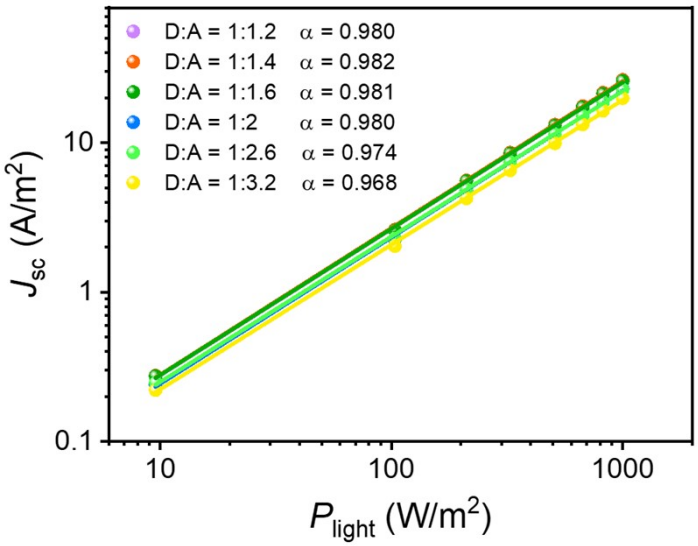

Fig. S23 J_{sc}-P_{light} plots for the PBDTTPTP:N3 solar cells with different D/A ratios.

13. P_{diss} and P_{coll}

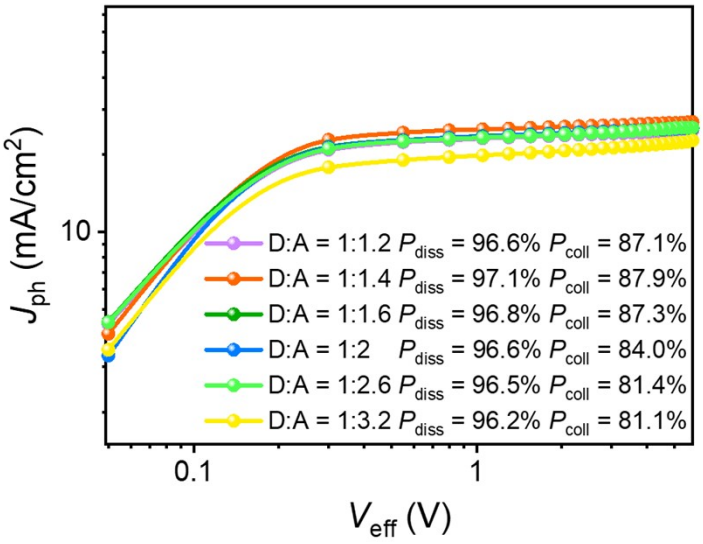

Fig. S24 J_{ph}-V_{eff} plots for the PBDTTPTP:N3 solar cells with different D/A ratios.

14. Optimization of Ag and Au thickness for PBDTTPTP:N3 semitransparent solar cells

Table S4 Optimization of Ag thickness for PBDTTPTP:N3 semitransparent solar cells.[a]

Thickness (Ag) [nm]	V_{oc} [V]	J_{sc} [mA/cm^2]	FF [%]	PCE [%]	AVT [%]	LUE [%]
10	0.827	18.44	66.2	10.10 (10.00)[b]	24.0	2.42
15	0.824	20.01	68.7	11.32 (11.29)	23.1	2.61
20	0.828	20.53	71.4	12.14 (12.03)	16.9	2.05
30	0.830	21.75	72.2	13.05 (12.91)	8.6	1.12

[a]D/A ratio: 1:2.6 (w:w); blend solution: 12 mg/mL in CF; Au is not used.
[b]Data in parentheses stand for the average PCEs for 10 cells.

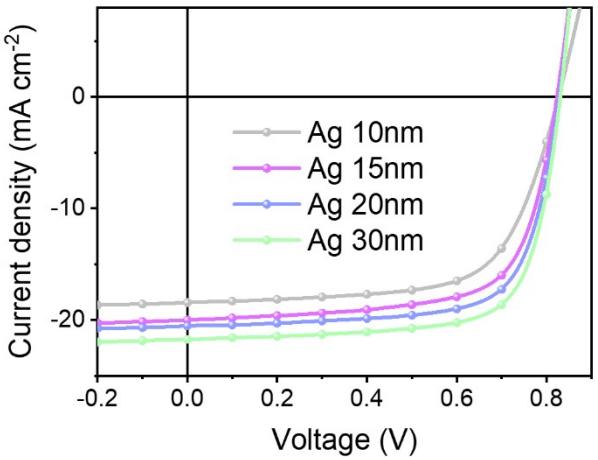

Fig. S25 *J-V* curves for PBDTTPTP:N3 semitransparent solar cells with varied Ag thicknesses.

Table S5 Optimization of Au thickness for PBDTTPTP:N3 semitransparent solar cells.[a]

Thickness (Au) [nm]	V_{oc} [V]	J_{sc} [mA/cm^2]	FF [%]	PCE [%]	AVT [%]	LUE [%]
0	0.824	20.01	68.7	11.32 (11.29)[b]	23.1	2.61
1	0.831	21.14	71.8	12.61 (12.21)	22.8	2.88
1.5	0.825	22.06	68.9	12.54 (12.02)	19.6	2.46

[a]D:A ratio: 1:2.6 (w:w); blend solution: 12 mg/mL in CF; the thickness of Ag is 15 nm.
[b]Data in parentheses stand for the average PCEs for 10 cells.

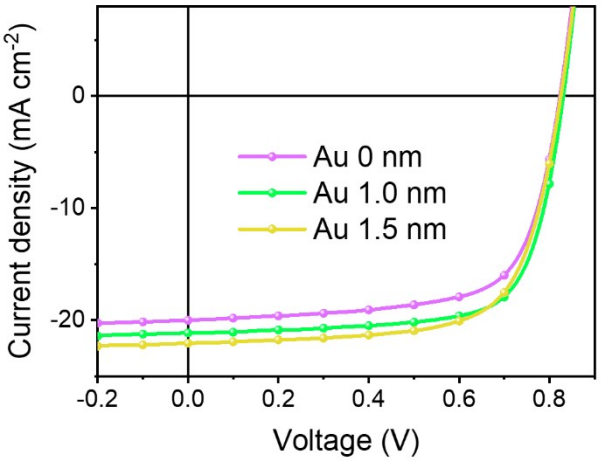

Fig. S26 *J-V* curves for PBDTTPTP:N3 semitransparent solar cells with varied Au thicknesses.

15. Optimization of ARC for PBDTTPTP:N3 semitransparent solar cells

Table S6 The performance of PBDTTPTP:N3 semitransparent solar cells with different ARC.[a]

ARC	V_{oc} [V]	J_{sc} [mA/cm^2]	FF [%]	PCE [%]	AVT [%]	LUE [%]
MgF_2 [c]	0.821	21.36	71.0	12.47 (12.34) [b]	26.7	3.33
MgF_2+MoO_3 [d]	0.828	20.65	71.7	12.26 (12.17)	35.7	4.38

[a]D/A ratio: 1:2.6 (w:w); blend solution: 12 mg/mL in CF.
[b]Data in parentheses stand for the average PCEs for 10 cells.
[c]Device structure: MgF_2 (100 nm)/glass/ITO/PEDOT:PSS/PBDTTPTP:N3/PDIN/Au (1 nm)/Ag (15 nm).
[d]Device structure: MgF_2 (100 nm)/glass/ITO/PEDOT:PSS/PBDTTPTP:N3/PDIN/Au (1 nm)/Ag (15 nm)/MoO_3 (35 nm).

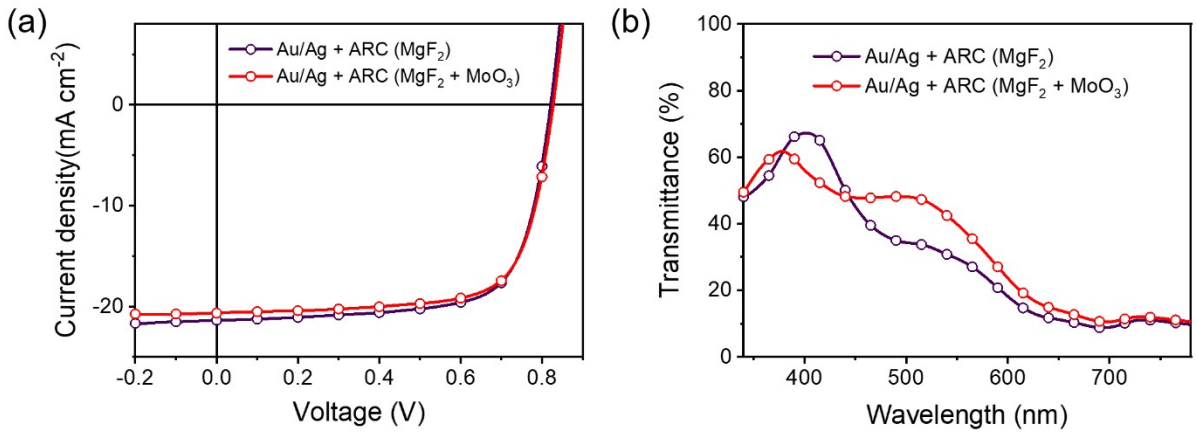

Fig. S27 (a) *J-V* curves and (b) transmittance spectra for PBDTTPTP:N3 semitransparent solar cells with different ARC.

16. EQE spectra for PBDTTPTP:N3 semitransparent solar cells with different D/A ratios

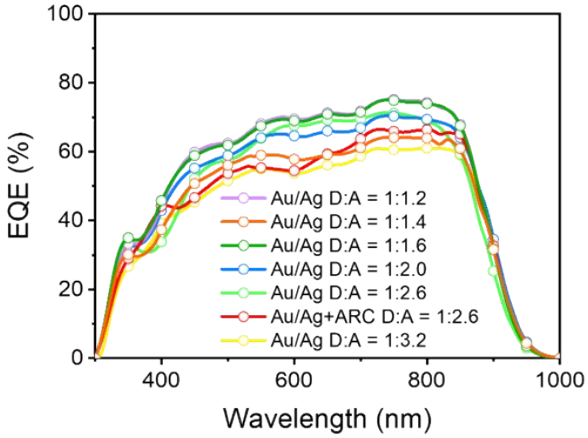

Fig. S28 EQE spectra for PBDTTPTP:N3 semitransparent solar cells with different D/A ratios.

17. Performance comparison for semitransparent solar cells based on PBDTTPTP and different acceptors.

Table S7 The performance of semitransparent solar cells based on PBDTTPTP and different acceptors.[a]

Acceptor	V_{oc} [V]	J_{sc} [mA/cm^2]	FF [%]	PCE [%]	AVT [%]	LUE [%]
N3	0.831	21.14	71.8	12.61 (12.21)[b]	22.8	2.88
Y6	0.835	18.71	71.2	11.13 (10.76)	19.0	2.11
BTP-eC9	0.849	20.35	70.5	12.18 (11.75)	18.2	2.22

[a]D:A ratio: 1:2.6 (w:w); blend solution: 12 mg/mL in CF; Device structure: glass/ITO/PEDOT:PSS/PBDTTPTP:acceptor/PDIN/Au (1 nm)/Ag (15 nm).
[b]Data in parentheses stand for the average PCEs for 10 cells.

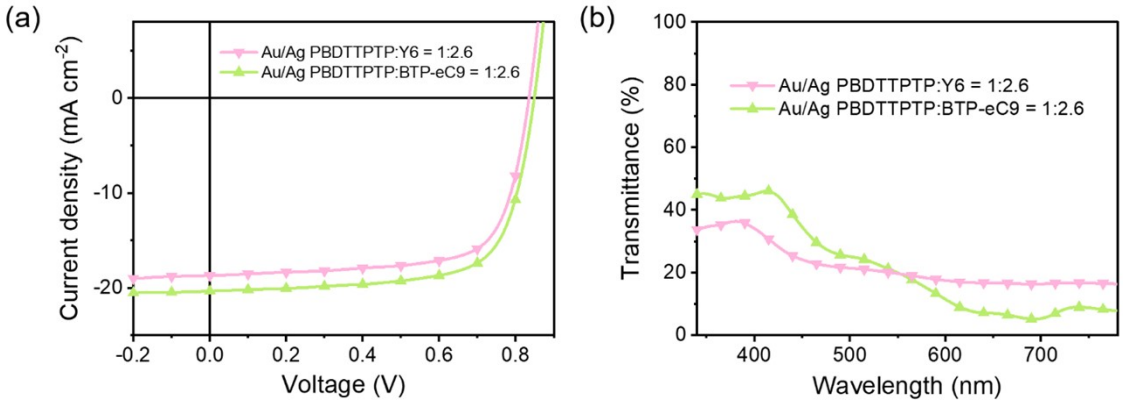

Fig. S29 (a) *J-V* curves and (b) transmittance spectra for PBDTTPTP:Y6 and PBDTTPTP:BTP-eC9 semitransparent solar cells.

18. Light-soaking stability test for PBDTTPTP:N3 opaque and semitransparent solar cells

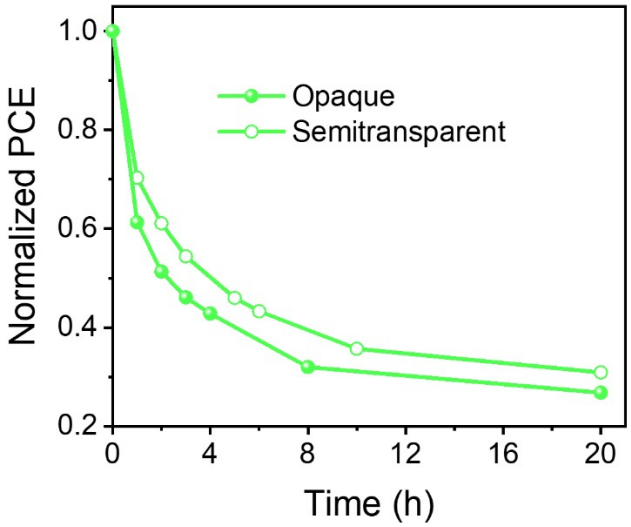

Fig. S30 Light-soaking stability test (1 sun irradiation) for opaque (Ag (80 nm)) and semitransparent (Au (1 nm)/Ag (15 nm)) PBDTTPTP:N3 cells with a D:A ratio of 1:2.6.

19. The performance of the 1 cm² PBDTTPTP:N3 semitransparent cells

Table S8 The performance of the 1 cm^2 PBDTTPTP:N3 semitransparent cells.[a]

D:A [w:w]	V_{oc} [V]	J_{sc} [mA/cm^2]	FF [%]	PCE [%]	AVT [%]	LUE [%]
1:2.6	0.838	23.80	57.2	11.40 (11.01)[b]	35.7	4.07

[a]Device structure: MgF_2 (100 nm)/glass/ITO/PEDOT:PSS/PBDTTPTP:N3/PDIN/Au (1 nm)/Ag (15 nm)/MoO_3 (35 nm).
[b]Data in parentheses stand for the average PCEs for 10 cells.

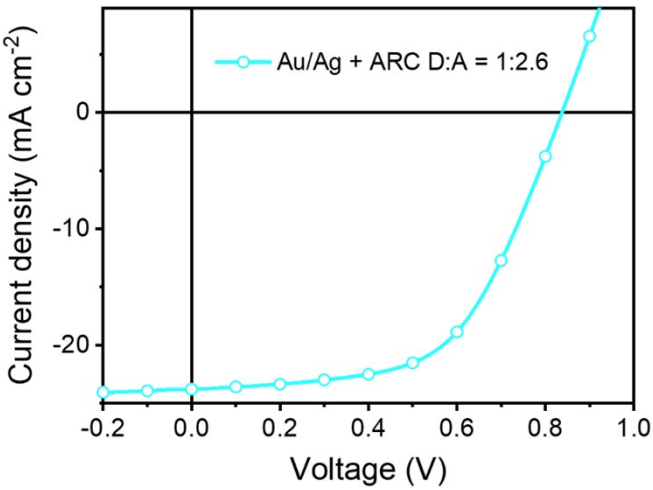

Fig. S31 *J-V* curve for the best 1 cm^2 semitransparent solar cell.

References

[1] N. Windmon and V. Dragojlovic, *Tetrahedron Lett.*, 2008, **49**, 6543-6546.

[2] K. Schuh and F. Glorius, *Synthesis*, 2007, **15**, 2297-2306.

[3] H. Bin, L. Gao, Z-G Zhang, Y. Yang, Y. Zhang, C. Zhang, S. Chen, L. Xue, C. Yang, M. Xiao and Y. Li, *Nat. Commun*., 2016, **7**, 13651.

[4] W. Yang, W. Wang, Y. Wang, R. Sun, J. Guo, H. Li, M. Shi, J. Guo, Y. Wu, T. Wang, G. Lu, C. J. Brabec, Y. Li and J. Min, *Joule*, 2021, **5**, 1209-1230.

[5] R. Po, G. Bianchi, C. Carbonera and A. Pellegrino, *Macromolecules*, 2015, **48**, 453–461.

[6] C. Yang, D. Liu, M. Bates, M. C. Barr and R. R. Lunt, *Joule*, 2019, **3**, 1803-1809.